Angle-resolved x-ray spectroscopic scheme to determine overlapping hyperfine splittings in highly charged heliumlike ions

Z. W. Wu,[1,2] A. V. Volotka,[1,3] A. Surzhykov,[4,5] and S. Fritzsche[1,6]

[1]*Helmholtz-Institut Jena, D-07743 Jena, Germany*

[2]*Key Laboratory of Atomic and Molecular Physics & Functional Materials of Gansu Province, College of Physics and Electronic Engineering, Northwest Normal University, Lanzhou 730070, People's Republic of China*

[3]*Department of Physics, St. Petersburg State University, 198504 St. Petersburg, Russia*

[4]*Physikalisch-Technische Bundesanstalt, D-38116 Braunschweig, Germany*

[5]*Technische Universität Braunschweig, D-38106 Braunschweig, Germany*

[6]*Theoretisch-Physikalisches Institut, Friedrich-Schiller-Universität Jena, D-07743 Jena, Germany*

(Received 3 April 2017; published 5 July 2017)

An angle-resolved x-ray spectroscopic scheme is presented for determining the hyperfine splitting of highly charged ions. For heliumlike ions, in particular, we propose to measure either the angular distribution or polarization of the $1s2p^3P_1, F \to 1s^2{}^1S_0, F_f$ emission following the stimulated decay of the initial $1s2s^1S_0, F_i$ level. It is found that both the angular and polarization characteristics of the emitted x-ray photons strongly depend on the (relative) *splitting* of the partially overlapping hyperfine $1s2p^3P_1, F$ resonances and may thus help resolve their hyperfine structure. The proposed scheme is feasible with present-day photon detectors and allows a measurement of the hyperfine splitting of heliumlike ions with a relative accuracy of about 10^{-4}.

DOI: 10.1103/PhysRevA.96.012503

I. INTRODUCTION

Hyperfine splitting of energy levels occurs primarily due to the interaction of bound electrons with the magnetic (dipole) field of nucleus. The strength of this nuclear magnetic field increases rapidly with the nuclear charge and reaches about 10^9 T at the surface of ^{209}Bi nucleus, several orders of magnitude higher than the field of the most powerful magnets. For this reason, the study of the hyperfine splitting in highly charged ions has attracted much recent attention from both theory and experiment, and aims to probe bound-state QED at extreme electric and magnetic fields. In the past, various high-precision measurements on the hyperfine splitting in hydrogenlike ions were performed [1–4] and thus stimulated a good deal of theoretical developments; see review [5] and references therein. Due to recent advances in experiment, moreover, the accuracy of the (measured) hyperfine splitting in ^{209}Bi^{82+} was improved by almost one order of magnitude and meanwhile reached the level of about 10^{-5} [6]. Until now, however, further theoretical progress has been restricted by the lack of knowledge of the nuclear magnetization distribution. In Ref. [7], it was therefore proposed to consider the specific difference of the hyperfine splitting in different electronic configurations, e.g., the difference between the ground-state hyperfine splitting in hydrogen- and lithiumlike ions of the same isotope, for which the uncertainty due to the nuclear magnetization distribution is substantially reduced.

Besides ground-state hyperfine splitting in hydrogenlike ions, until now only a very few measurements have been made for lithium- and berylliumlike praseodymium ions [8] and lithiumlike bismuth ions [9]. Recently, the LiBELLE collaboration presented a new high-precision measurement of the ground-state hyperfine splitting in ^{209}Bi^{80+} ion [10]. The specific difference between the hyperfine splitting in hydrogen- and lithiumlike bismuth ions, determined in this measurement, yields 7σ disagreement when compared with the corresponding theoretical values [11]. In order to resolve this discrepancy, additional measurements of the hyperfine splitting with different electronic configurations are highly desirable.

Heliumlike ions are another alternative that may serve for the same purpose. Apart from the hyperfine quenching (cf. the review by Johnson [12]), however, to the best of our knowledge there are no experimental studies on the hyperfine structure of such ions. In contrast to hydrogen- and lithiumlike ions, there is no hyperfine splitting in the $1s^2{}^1S_0, F_f$ ground level of heliumlike ions. As for the excited levels $1s2p^{1,3}P_1, F$ (and $1s2s^3S_1, F'$), for which the natural linewidth is comparable in magnitude or even larger than the corresponding hyperfine splitting, they can therefore not be resolved by conventional fluorescence spectroscopy. For the $1s2p^3P_1, F$ levels, for example, the natural linewidth goes rapidly from 0.10 eV for ^{71}Ga^{29+} to 12.75 eV for ^{209}Bi^{81+}, while the hyperfine splitting just increases from 0.11 eV to 5.35 eV. Moreover, the transition energies of the (partially) overlapping $1s2p^3P_1, F$ levels to the ground state are quite large and thus less suitable for precision measurements.

In this contribution, we propose a scheme for resolving the hyperfine splitting in highly charged heliumlike ions by measuring the angular distribution and angle-resolved polarization of the emitted fluorescence photons. As an example, we shall predict and analyze the angular distribution and linear polarization of the γ_2 photons emitted in the two-step radiative decay

$$1s2s^1S_0, F_i + \gamma_1 \longrightarrow 1s2p^3P_1, F \longrightarrow 1s^2{}^1S_0, F_f + \gamma_2 \qquad (1)$$

of heliumlike ions, from which we aim to determine the hyperfine splitting of the intermediate $1s2p^3P_1, F$ levels. Figure 1 displays the (involved) fine-structure levels of heliumlike ^{71}Ga^{29+} ions and their hyperfine splittings (left panel). In this scheme, the ions first decay from the initial $1s2s^1S_0, F_i$ level to the intermediate $1s2p^3P_1, F$ levels under a stimulation by incident laser photons γ_1. Subsequently, fast

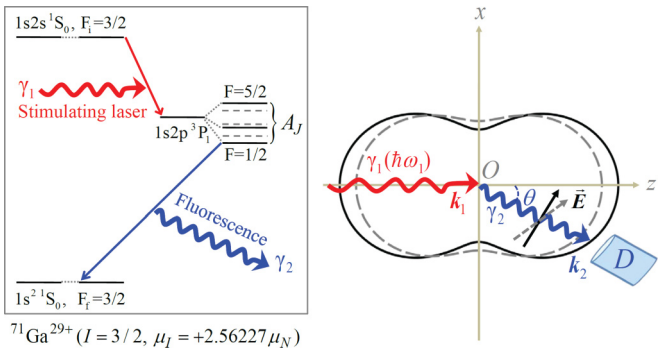

FIG. 1. Schema (left panel) and geometry (right panel) for measuring the two-step radiative decay (1) of heliumlike $^{71}Ga^{29+}$ ions. While the first-step decay is stimulated by laser photons γ_1 with energy $\hbar\omega_1$, the fast subsequent spontaneous decay to the $1s^2\,^1S_0, F_f$ ground level gives rise to an emission of the γ_2 fluorescence photons. As distinguished in black solid and gray dashed lines, the angular distribution and polarization of the γ_2 photons depend sensitively on the hyperfine constant of the intermediate levels.

spontaneous decay of the $1s2p^3P_1, F$ levels into the ground level $1s^2\,^1S_0, F_f$ occurs with an emission of the γ_2 photons. The angular distribution and polarization of the emitted γ_2 photons are then measured as functions of the photon energy $\hbar\omega_1$. The obtained γ_2 angular distribution and polarization are expected to be sensitive to the $1s2p^3P_1, F$ hyperfine splittings due to their different populations following the first-step stimulated decay, as shown in the right panel of Fig. 1.

It is well known, both experimentally [13] and theoretically [14,15], that the angular distribution and polarization of $K\alpha_1$ photons in heliumlike ions are often affected by the hyperfine admixture of different fine-structure levels, which may alter the branching ratios between different hyperfine sublevels. In the proposed scheme, the hyperfine levels can be populated in a controlled manner by just tuning the photon energy $\hbar\omega_1$ of the incident laser over the resonance of the first-step decay. By analyzing the angular distribution or linear polarization of the emitted γ_2 fluorescence photons, one can restore the created population. Below, we will demonstrate that the angular distribution and polarization of the γ_2 photons depend sensitively on the hyperfine splitting, as shown in the right panel of Fig. 1. The obtained results suggest that an angle- or polarization-resolved measurement of the $1s2p^3P_1, F \to 1s^2\,^1S_0, F_f$ emission line may provide an experimental determination on the splitting of the partially overlapping hyperfine levels with a relative accuracy of about 10^{-4}.

II. THEORETICAL BACKGROUND

To understand how the splitting of overlapping hyperfine levels affect the fluorescence emission of heliumlike ions, let us start from a theoretical analysis of the photon angular distribution and linear polarization. Our theory is developed within the framework of density matrix and second-order perturbation theory. For the two-step decay process (1), if the geometry in Fig. 1 is adopted, the second-order transition amplitudes can be expressed in the form [16]

$$\mathcal{M}^{\lambda_1,\lambda_2}_{M_i,M_f}(\hbar\omega_1) = \sum_{FM}\sum_{p_1 L_1 M_{L_1}}\sum_{p_2 L_2 M_{L_2}} i^{-L_1-L_2}\,(i\lambda_1)^{p_1}\,(i\lambda_2)^{p_2}\,\delta_{\lambda_1 M_{L_1}}\,D^{L_2}_{M_{L_2}\lambda_2}(\varphi,\theta,0)\,[L_1,L_2]^{1/2}\,[F_i,F]^{-1/2}\,(-1)^{F_i-F_f}$$
$$\times\langle F_f M_f, L_2 M_{L_2}|FM\rangle\,\langle FM, L_1 M_{L_1}|F_i M_i\rangle\,\frac{\langle F_f\|\sum_m \boldsymbol{\alpha}_m \boldsymbol{a}^{p_2}_{L_2}(\boldsymbol{r}_m)\|F\rangle\langle F\|\sum_m \boldsymbol{\alpha}_m \boldsymbol{a}^{p_1}_{L_1}(\boldsymbol{r}_m)\|F_i\rangle}{E_{F_i}-E_F-\hbar\omega_1+i\,\Gamma_F/2}. \quad (2)$$

Here, $\delta_{\lambda_1 M_{L_1}}$ denotes a Kronecker delta function, $[a,b]\equiv(2a+1)(2b+1)$, and the standard notations for the Wigner D functions and the Clebsch-Gordan coefficients have been employed. Moreover, the individual photons $\gamma_{1,2}$ are characterized in terms of their helicity λ and multipolarities pL, with $p=0$ for magnetic multipoles and $p=1$ for electric ones. E_F and Γ_F represent, respectively, the energy and natural linewidth of the hyperfine level $|F\rangle\equiv|\alpha JIF\rangle$ with (total) angular momentum F, nuclear spin I, angular momentum J of the electronic state, and all additional quantum numbers α that are needed for its unique specification. It should be noted that, we here neglect the linewidth Γ_{F_i} of the initial level in the denominator as it is much smaller than the linewidth Γ_F of the intermediate levels. The hyperfine transition amplitudes $\langle F'\|\sum_m \boldsymbol{\alpha}_m \boldsymbol{a}^p_L(\boldsymbol{r}_m)\|F\rangle$ can be obtained from the corresponding fine-structure transition amplitudes by representing the IJ coupled atomic basis states in their product basis. From the hyperfine transition amplitudes, we can easily determine the decay rate of excited hyperfine-resolved levels and their natural linewidths. The transition amplitudes of the $1s2s\,^1S_0 \to 1s2p^3P_1$ and $1s2p^3P_1 \to 1s^2\,^1S_0$ are here evaluated within the framework of perturbation theory and by including the first-order interelectronic-interaction correction; see Ref. [17] for details. For the case of the transition $1s2p^3P_1 \to 1s^2\,^1S_0$, the obtained results agree fairly with previously published values [18–20].

Apart from the hyperfine transition amplitudes and natural linewidths Γ_F, we still need to know the hyperfine structure energies in order to compute the second-order transition amplitudes (2). Since the electric-quadrupole hyperfine interactions are negligibly small throughout the heliumlike isoelectronic sequence when compared to the nuclear magnetic-dipole interaction, they will not be considered here. The magnetic-dipole hyperfine splitting of a fine-structure level αJ can be expressed as

$$\Delta E^{\rm hf}_{\alpha JIF} = A_J[F(F+1)-I(I+1)-J(J+1)]/2 \quad (3)$$

in terms of the hyperfine constant A_J. With this notation, $E_F = E_{\alpha J} + \Delta E^{\rm hf}_{\alpha JIF}$, where $E_{\alpha J}$ is the energy of the corresponding fine-structure level. As seen from Eq. (3), the hyperfine splitting can be easily obtained once the hyperfine constant is determined. The hyperfine constant of the $1s2p^3P_1$ level

TABLE I. Table of isotopes with nuclear spin I and magnetic moment μ_I in units of the nuclear magneton μ_N considered in this work [24]. The calculated hyperfine constant A_J (eV) and natural linewidth Γ_F (eV) of the $1s2p^3P_1$ level are presented, together with the transition energies (eV) of both the $1s2s^1S_0 \rightarrow 1s2p^3P_1$ and $1s2p^3P_1 \rightarrow 1s^21S_0$ lines taken from Ref. [25]. The anisotropy and polarization sensitivity coefficients $\frac{d\beta}{dA_J}\frac{A_J}{\beta}$ and $\frac{dP_1}{dA_J}\frac{A_J}{P_1}$ are calculated at the resonance energies.

Isotope ^AX	Spin I	Magnetic moment μ_I	Hyperfine constant $A_J\,(2^3P_1)$	Linewidth $\Gamma_F\,(2^3P_1)$	Transition energies $2^1S_0 \rightarrow 2^3P_1$	Transition energies $2^3P_1 \rightarrow 1^1S_0$	$\frac{d\beta}{dA_J}\frac{A_J}{\beta}$	$\frac{dP_1}{dA_J}\frac{A_J}{P_1}$
$^{71}Ga^{29+}$	3/2	+2.56227	0.0274	0.1012	0.173	9574.446	−1.184	−1.356
$^{141}Pr^{57+}$	5/2	+4.2754	0.2530	2.9551	12.461	36391.292	−0.400	−0.499
$^{209}Bi^{81+}$	9/2	+4.1103	0.5349	12.7539	63.961	76131.359	−0.291	−0.369

is evaluated in the intermediate coupling scheme of mixing $1s2p^3P_1$ and $1s2p^1P_1$ levels as in Ref. [21], while the remaining interelectronic-interaction corrections are accounted for by a local screening potential. The effect of nuclear magnetization distribution is calculated by employing the nuclear single-particle model [22]. The obtained hyperfine constants are in fair agreement with the results from Ref. [23]. In addition, we also estimate the one-electron QED corrections—self-energy and vacuum polarization—to the hyperfine constant A_J. These corrections contribute, for instance, about 0.5% for $^{209}Bi^{81+}$ ions.

As an attempt on this kind of study, the incident stimulating laser is assumed to be unpolarized for simplicity. In this case, the density matrix of the emitted γ_2 photons can be expressed in terms of the second-order amplitudes (2) as follows:

$$\rho^{\gamma_2}_{\lambda_2,\lambda_2'} \equiv \langle \hat{\boldsymbol{k}}_2,\lambda_2|\rho^{\gamma_2}|\hat{\boldsymbol{k}}_2,\lambda_2'\rangle = \frac{1}{2[F_i]}\sum_{M_i,M_f}\sum_{\lambda_1=\pm1}\mathcal{M}^{\lambda_1,\lambda_2}_{M_i,M_f}(\hbar\omega_1)\mathcal{M}^{\lambda_1,\lambda_2'*}_{M_i,M_f}(\hbar\omega_1)\,. \tag{4}$$

Once we obtain the density matrix (4), the angular distribution and polarization of the γ_2 photons can be given in terms of its matrix elements. If, for instance, the polarization of the γ_2 photons remains unobserved, the γ_2 angular distribution follows simply from the trace of Eq. (4),

$$\frac{d\sigma}{d\Omega} = \rho^{\gamma_2}_{+1,+1} + \rho^{\gamma_2}_{-1,-1} = \frac{\sigma_0}{4\pi}[1+\beta P_2(\cos\theta)]\,. \tag{5}$$

As the γ_1 photons are unpolarized, the angular distribution (5) is azimuthally symmetric and thus independent of the angle φ. For this reason, it is parametrized by a single, so-called *anisotropy* parameter β within the $E1$ approximation, as shown in the second equality. Moreover, the linear polarization P_1 can be given as follows:

$$P_1 = (\rho^{\gamma_2}_{+1,-1} + \rho^{\gamma_2}_{-1,+1})/(\rho^{\gamma_2}_{+1,+1} + \rho^{\gamma_2}_{-1,-1})\,. \tag{6}$$

We are now ready to study the angular distribution and linear polarization of the emitted γ_2 photons.

III. RESULTS AND DISCUSSION

Table I lists the calculated hyperfine constant and linewidth of the $1s2p^3P_1$ level, together with the transition energies of the $1s2s^1S_0 \rightarrow 1s2p^3P_1$ and $1s2p^3P_1 \rightarrow 1s^21S_0$ lines from Ref. [25] for heliumlike $^{71}Ga^{29+}$, $^{141}Pr^{57+}$, and $^{209}Bi^{81+}$ ions. These data are used for the evaluation of the second-order transition amplitudes and, further, to analyze the angular distribution and linear polarization of the emitted γ_2 photons. Figure 2 displays the anisotropy parameter β and the linear polarization P_1 of the $1s2p^3P_1, F = 1/2,3/2,5/2 \rightarrow 1s^21S_0, F_f = 3/2$ fluorescence photons of heliumlike $^{71}Ga^{29+}$ ions as functions of the photon energy $\hbar\omega_1$. The linear polarization P_1 is presented for the γ_2 photons that are emitted perpendicular to the incident γ_1 photons, i.e., at $\theta = 90^\circ$. The parameter $P_1 = (I_{0^\circ} - I_{90^\circ})/(I_{0^\circ} + I_{90^\circ})$ characterizes the intensities of the emitted γ_2 photons linearly polarized in parallel (I_{0°) or perpendicular (I_{90°) to the reaction plane defined by the propagation directions of the γ_1 and γ_2 photons. Results are shown for the calculated hyperfine constant $A_J = 0.0274$ eV and also for two assumed values, $0.8A_J$ and $1.2A_J$, which differ by just 20%.

As can be seen from the figure, both the γ_2 anisotropy and linear polarization appear to be rather sensitive with regard to the photon energy $\hbar\omega_1$ for any given hyperfine constant of the $1s2p^3P_1, F$ levels. Typically, the γ_2 photons have the smallest anisotropy and polarization near the resonance energy $\hbar\omega_1 \simeq 0.173$ eV, but both become more and more anisotropic or (linearly) polarized when the photon energy $\hbar\omega_1$ is tuned away from the resonance. This dependence arises from

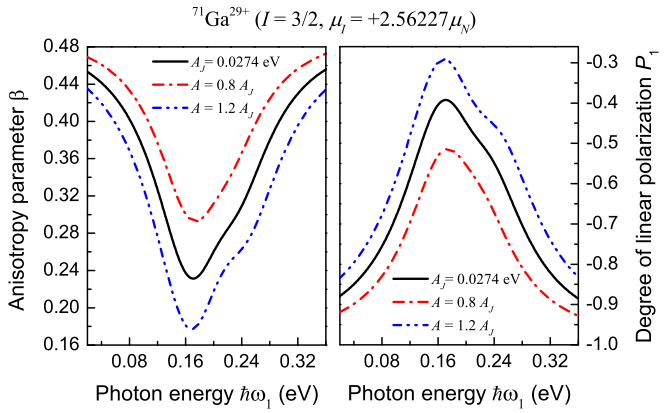

FIG. 2. Anisotropy parameter β (left panel) and degree of linear polarization P_1 (right panel) of the hyperfine $1s2p^3P_1, F = 1/2,3/2,5/2 \rightarrow 1s^21S_0, F_f = 3/2$ fluorescence emission from heliumlike $^{71}Ga^{29+}$ ions as functions of photon energy $\hbar\omega_1$ of the incident photons γ_1. Results are shown for the calculated hyperfine constant $A_J = 0.0274$ eV (black solid lines) as listed in Table I as well as for two assumed values, $0.8A_J$ (red dash-dotted lines) and $1.2A_J$ (blue dash-dot-dotted lines), which differ by just 20%.

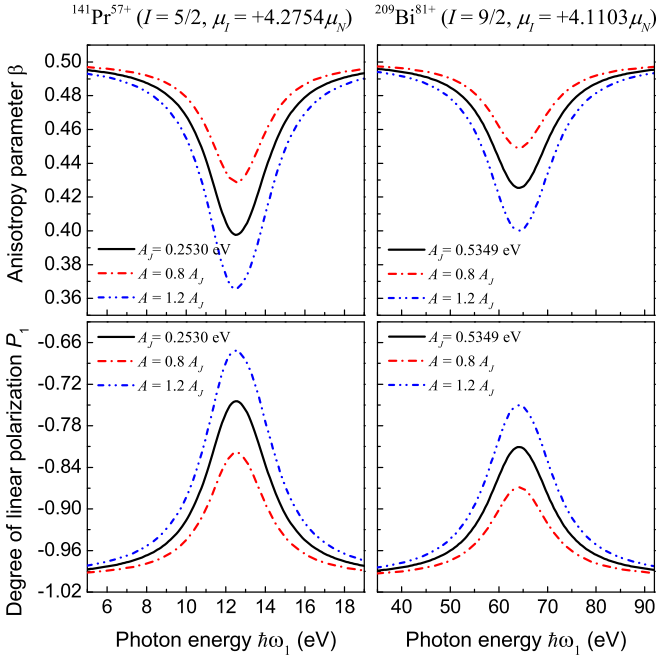

FIG. 3. Same as in Fig. 2 but for $^{141}Pr^{57+}$ (left panel) and $^{209}Bi^{81+}$ (right panel) ions.

the finite linewidths of the overlapping resonances $1s2p^3P_1$, $F = 1/2,3/2,5/2$, which lead to a coherent population of them during the first-step stimulated decay and, ultimately, affects the angular and polarization behaviors of the emitted γ_2 photons. Moreover, both the anisotropy parameter and linear polarization depend strongly on the hyperfine constant of the $1s2p^3P_1$ level, especially, if the γ_1 photon energy is close to the resonance, say, $\hbar\omega_1 \simeq 0.173$ eV. The linear polarization P_1, for instance, changes from -0.39 for $A_J = 0.0274$ eV to -0.51 for $0.8A_J$ at this resonance energy. In order to further analyze this dependence quantitatively, two sensitivity coefficients $\frac{d\beta}{dA_J}\frac{A_J}{\beta}$ and $\frac{dP_1}{dA_J}\frac{A_J}{P_1}$ are introduced. These coefficients reach their respective maximums at the resonance energy, which are listed in Table I. From these coefficients, it is quite easy to see how a change in the hyperfine constant A_J will affect the γ_2 anisotropy or polarization, i.e., if A_J is modified by, say, 20%, β will change by 23.6%, while P_1 by 27.2%, as shown in Fig. 2.

Besides the low-Z $^{71}Ga^{29+}$, we also consider medium- and high-Z ions such as $^{141}Pr^{57+}$ and $^{209}Bi^{81+}$. For these ions, the corresponding γ_2 anisotropy and linear polarization still depend on the $1s2p^3P_1,F$ hyperfine splittings and also on the photon energy $\hbar\omega_1$, as shown in Fig. 3, although this dependence is slightly reduced when compared to the case of $^{71}Ga^{29+}$. In practice, this dependence arises from the interplay of the lifetime and splitting of the hyperfine levels that contribute to the γ_2 emission, and it becomes strongest when the splitting and linewidths are comparable in magnitude. For both $^{141}Pr^{57+}$ and $^{209}Bi^{81+}$ ions, moreover, the corresponding sensitivity coefficients are also given in Table I. The obtained strong angular and polarization dependence of the emitted γ_2 photons on the hyperfine constant is therefore expected to help determine the hyperfine splitting of highly charged heliumlike ions.

IV. EXPERIMENTAL FEASIBILITY

The proposed scheme is feasible with present-day experimental facilities, such as heavy-ion storage rings or electron-beam ion traps. The initial $1s2s^1S_0$ level can be populated quite selectively via K-shell ionization of lithiumlike projectiles in relativistic collisions with gas target at the experimental storage ring [26–28]. Alternatively, it can also be populated via the prompt $2s2p^1P_1 \rightarrow 1s2s^1S_0$ decay following the resonant electron capture of hydrogenlike ions into the $2s2p^1P_1$ resonance [29]. Due to the high selectivity on the production of the $1s2s^1S_0$ level, as demonstrated in these experiments, the influence of neighboring levels on its subsequent decay can be ignored.

The $1s2s^1S_0,F_i$ level of heliumlike ions is known to decay primarily into the $1s^21S_0,F_f$ ground level via two-photon ($2E1$) emission [30]. Since we wish to study the effect of the $1s2p^3P_1,F$ hyperfine splitting upon the angular distribution and linear polarization of the emitted γ_2 photons, cf. Fig. 1, our aim is to make the $1s2s^1S_0,F_i \rightarrow 1s2p^3P_1,F$ transition strong enough to compete with the $2E1$ decay and thus to populate the $1s2p^3P_1,F$ levels. For this aim, this transition is supposed to be stimulated by the incident laser photons γ_1 with suitable intensity and tunable energy $\hbar\omega_1$. For $^{71}Ga^{29+}$ ions, for example, we obtain the required minimum laser intensity 3.2×10^5 W/cm^2 by using Eq. (35) in Ref. [31]. For both $^{141}Pr^{57+}$ and $^{209}Bi^{81+}$ ions, in addition, the corresponding minimum intensities are also determined in a similar way to be 3.0×10^9 W/cm^2 and 3.6×10^{11} W/cm^2, respectively. For such low laser intensities, the resulting Stark effect on the energy levels of ions is negligibly small and hence can be ignored. These intensities are easily accessible with present-day laser sources from near-infrared to extreme-ultraviolet photon energy regions. Since the linewidth of laser radiations in this energy range is much smaller than the natural linewidth of the levels involved, the incident stimulating laser photons γ_1 can be treated to be monochromatic.

Finally, let us discuss the measurement of the angular distribution and linear polarization of the emitted γ_2 fluorescence photons. The angular distribution can be accurately measured by an array of highly efficient solid-state Ge(i) detectors placed at different angles, while the polarization can be determined by means of two-dimensional position-sensitive x-ray detectors and Compton scattering technique [32,33]. Moreover, due to recent progress in the channel-cut silicon crystal polarimetry technique the polarization purity of x-ray photons have been measured with an unprecedented level of accuracy, $\sim 10^{-10}$ [34]. Since the required emission flux of the γ_2 photons for achieving such a high accuracy is mainly restricted by the amount of the production of heliumlike ions, we may thus expect an experimental uncertainty of about 10^{-4} in measuring the anisotropy parameter β and the polarization P_1. This uncertainty allows one to determine the hyperfine constant on a level of accuracy 7×10^{-5} for $^{71}Ga^{29+}$ and of 3×10^{-4} for $^{209}Bi^{81+}$, which would be well below the level of the contributing QED effects.

In summary, the angular distribution and linear polarization of x-ray photons emitted in a two-step radiative decay of highly charged heliumlike ions have been studied with the aim to pursue a scheme for determining their hyperfine splitting. For the particular process (1), it is found that the angular and

polarization behaviors of the γ_2 photons depend strongly on the hyperfine splitting of the $1s2p^3P_1, F$ levels. This dependence will allow a determination on the hyperfine splitting of heliumlike ions with an accuracy of about 10^{-4}, together with the hyperfine structures of hydrogen- and lithiumlike ions which could serve as a probe of QED in strong electromagnetic field generated by heavy nuclei.

ACKNOWLEDGMENTS

We are grateful to S. Trotsenko and B. Marx for very helpful discussions on the production of highly charged ion beam and high-precision x-ray polarization measurement, respectively. This work has been supported by the BMBF (Grant No. 05P15SJFAA) and the NSFC (Grants No. 11464042 and No. U1332206).

[1] I. Klaft, S. Borneis, T. Engel, B. Fricke, R. Grieser, G. Huber, T. Kühl, D. Marx, R. Neumann, S. Schröder, P. Seelig, and L. Völker, Phys. Rev. Lett. **73**, 2425 (1994).

[2] J. R. Crespo López-Urrutia, P. Beiersdorfer, D. W. Savin, and K. Widmann, Phys. Rev. Lett. **77**, 826 (1996); J. R. Crespo López-Urrutia, P. Beiersdorfer, K. Widmann, B. B. Birkett, A.-M. Mårtensson-Pendrill, and M. G. H. Gustavsson, Phys. Rev. A **57**, 879 (1998).

[3] P. Seelig, S. Borneis, A. Dax, T. Engel, S. Faber, M. Gerlach, C. Holbrow, G. Huber, T. Kühl, D. Marx, K. Meier, P. Merz, W. Quint, F. Schmitt, M. Tomaselli, L. Völker, H. Winter, M. Würtz, K. Beckert, B. Franzke, F. Nolden, H. Reich, M. Steck, and T. Winkler, Phys. Rev. Lett. **81**, 4824 (1998).

[4] P. Beiersdorfer, S. B. Utter, K. L. Wong, J. R. Crespo López-Urrutia, J. A. Britten, H. Chen, C. L. Harris, R. S. Thoe, D. B. Thorn, E. Träbert, M. G. H. Gustavsson, C. Forssén, and A. M. Mårtensson-Pendrill, Phys. Rev. A **64**, 032506 (2001).

[5] A. V. Volotka *et al.*, Ann. Phys. (Berlin) **525**, 636 (2013).

[6] J. Ullmann *et al.*, J. Phys. B **48**, 144022 (2015).

[7] V. M. Shabaev, A. N. Artemyev, V. A. Yerokhin, O. M. Zherebtsov, and G. Soff, Phys. Rev. Lett. **86**, 3959 (2001).

[8] P. Beiersdorfer, E. Träbert, G. V. Brown, J. Clementson, D. B. Thorn, M. H. Chen, K. T. Cheng, and J. Sapirstein, Phys. Rev. Lett. **112**, 233003 (2014).

[9] M. Lochmann, R. Jöhren, C. Geppert, Z. Andelkovic, D. Anielski, B. Botermann, M. Bussmann, A. Dax, N. Frommgen, M. Hammen, V. Hannen, T. Kühl, Y. A. Litvinov, R. López-Coto, T. Stöhlker, R. C. Thompson, J. Vollbrecht, A. Volotka, C. Weinheimer, W. Wen, E. Will, D. Winters, R. Sánchez, and W. Nortershäuser, Phys. Rev. A **90**, 030501(R) (2014).

[10] J. Ullmann *et al.*, Nat. Commun. **8**, 15484 (2017).

[11] A. V. Volotka, D. A. Glazov, O. V. Andreev, V. M. Shabaev, I. I. Tupitsyn, and G. Plunien, Phys. Rev. Lett. **108**, 073001 (2012).

[12] W. R. Johnson, Can. J. Phys. **89**, 429 (2011).

[13] J. R. Henderson, P. Beiersdorfer, C. L. Bennett, S. Chantrenne, D. A. Knapp, R. E. Marrs, M. B. Schneider, K. L. Wong, G. A. Doschek, J. F. Seely, C. M. Brown, R. E. LaVilla, J. Dubau, and M. A. Levine, Phys. Rev. Lett. **65**, 705 (1990).

[14] Z. W. Wu, A. Surzhykov, and S. Fritzsche, Phys. Rev. A **89**, 022513 (2014).

[15] A. Surzhykov, Y. Litvinov, Th. Stöhlker, and S. Fritzsche, Phys. Rev. A **87**, 052507 (2013).

[16] Z. W. Wu, A. V. Volotka, A. Surzhykov, C. Z. Dong, and S. Fritzsche, Phys. Rev. A **93**, 063413 (2016).

[17] P. Indelicato, V. M. Shabaev, and A. V. Volotka, Phys. Rev. A **69**, 062506 (2004).

[18] G. W. F. Drake, Phys. Rev. A **19**, 1387 (1979).

[19] W. R. Johnson, D. R. Plante, and J. Sapirstein, Adv. At. Mol. Opt. Phys. **35**, 255 (1995).

[20] O. Yu. Andreev, L. N. Labzowsky, and G. Plunien, Phys. Rev. A **79**, 032515 (2009).

[21] A. V. Volotka, V. M. Shabaev, G. Plunien, G. Soff, and V. A. Yerokhin, Can. J. Phys. **80**, 1263 (2002).

[22] V. M. Shabaev, M. Tomaselli, T. Kühl, A. N. Artemyev, and V. A. Yerokhin, Phys. Rev. A **56**, 252 (1997).

[23] W. R. Johnson, K. T. Cheng, and D. R. Plante, Phys. Rev. A **55**, 2728 (1997).

[24] N. J. Stone, At. Data Nucl. Data Tables **90**, 75 (2005).

[25] A. N. Artemyev, V. M. Shabaev, V. A. Yerokhin, G. Plunien, and G. Soff, Phys. Rev. A **71**, 062104 (2005).

[26] S. Fritzsche, P. Indelicato, and Th. Stöhlker, J. Phys. B **38**, S707 (2005).

[27] J. Rzadkiewicz, T. Stöhlker, D. Banaś, H. F. Beyer, F. Bosch, C. Brandau, C. Z. Dong, S. Fritzsche, A. Gojska, A. Gumberidze, S. Hagmann, D. C. Ionescu, C. Kozhuharov, T. Nandi, R. Reuschl, D. Sierpowski, U. Spillmann, A. Surzhykov, S. Tashenov, M. Trassinelli, and S. Trotsenko, Phys. Rev. A **74**, 012511 (2006).

[28] S. Trotsenko, A. Kumar, A. V. Volotka, D. Banaś, H. F. Beyer, H. Bräuning, S. Fritzsche, A. Gumberidze, S. Hagmann, S. Hess, P. Jagodziński, C. Kozhuharov, R. Reuschl, S. Salem, A. Simon, U. Spillmann, M. Trassinelli, L. C. Tribedi, G. Weber, D. Winters, and T. Stöhlker, Phys. Rev. Lett. **104**, 033001 (2010).

[29] P. H. Mokler, S. Reusch, A. Warczak, Z. Stachura, T. Kambara, A. Muller, R. Schuch, and M. Schulz, Phys. Rev. Lett. **65**, 3108 (1990).

[30] A. V. Volotka, A. Surzhykov, V. M. Shabaev, and G. Plunien, Phys. Rev. A **83**, 062508 (2011).

[31] F. Ferro, A. Surzhykov, and Th. Stöhlker, Phys. Rev. A **83**, 052518 (2011).

[32] S. Tashenov, T. Stöhlker, D. Banaś, K. Beckert, P. Beller, H. F. Beyer, F. Bosch, S. Fritzsche, A. Gumberidze, S. Hagmann, C. Kozhuharov, T. Krings, D. Liesen, F. Nolden, D. Protic, D. Sierpowski, U. Spillmann, M. Steck, and A. Surzhykov, Phys. Rev. Lett. **97**, 223202 (2006); S. Tashenov, T. Bäck, R. Barday, B. Cederwall, J. Enders, A. Khaplanov, Yu. Poltoratska, K.-U. Schässburger, and A. Surzhykov, *ibid.* **107**, 173201 (2011).

[33] G. Weber, H. Bräuning, A. Surzhykov, C. Brandau, S. Fritzsche, S. Geyer, S. Hagmann, S. Hess, C. Kozhuharov, R. Martin, N. Petridis, R. Reuschl, U. Spillmann, S. Trotsenko, D. F. A. Winters, and T. Stöhlker, Phys. Rev. Lett. **105**, 243002 (2010).

[34] B. Marx, K. S. Schulze, I. Uschmann, T. Kämpfer, R. Lötzsch, O. Wehrhan, W. Wagner, C. Detlefs, T. Roth, J. Härtwig, E. Förster, T. Stöhlker, and G. G. Paulus, Phys. Rev. Lett. **110**, 254801 (2013).